Scanning From Heating: 3D shape estimation of transparent objects from local surface heating

Gonen Eren[12], Olivier Aubreton[1], Fabrice Meriaudeau[1], L.A. Sanchez Secades[1], David Fofi[1], A. Teoman Naskali[2], Frederic Truchetet[1] and Aytul Ercil[2]

[1]*University of Burgundy, Le2i Laboratory CNRS UMR 5158, 12 rue de la Fonderie, 71200, Le Creusot, France*

[2]*Sabanci University, VPA Laboratory, Orhanli-Tuzla, 34956, Istanbul, Turkey*

gonenеren@su.sabanciuniv.edu

Abstract: Today, with quality becoming increasingly important, each product requires three-dimensional in-line quality control. On the other hand, the 3D reconstruction of transparent objects is a very difficult problem in computer vision due to transparency and specularity of the surface. This paper proposes a new method, called Scanning From Heating (SFH), to determine the surface shape of transparent objects using laser surface heating and thermal imaging. Furthermore, the application to transparent glass is discussed and results on different surface shapes are presented.

OCIS codes: (110.3080) Infrared imaging, (100.6890) Three-dimensional image processing, (100.2960) Image analysis, (330.7310) Vision, (140.3470) Lasers, carbon dioxide, (160.2750) Glass and other amorphous materials.

References and links

1. I. Ihrke, K. N. Kutulakos, H. P. A. Lensch, M. Magnor, and W. Heidrich, "State of the Art in Transparent and Specular Object Reconstruction," in *STAR Proceedings of Eurographics*, pp. 87–108 (2008).
2. S. Hata, Y. Saitoh, S. Kumamura, and K. Kaida, "Shape extraction of transparent object using genetic algorithm," in *Pattern Recognition, 1996., Proceedings of the 13th International Conference on*, vol. 4, pp. 684–688 (1996).
3. M. Ben-Ezra and S. Nayar, "What does motion reveal about transparency?" in *Ninth IEEE International Conference on Computer Vision*, vol. 2, pp. 1025–1032 (2003).
4. S. Agarwal, S. P. Mallick, D. Kriegman, and S. Belongie, "On refractive optical flow," in *ECCV'04, 8th European Conference on Computer Vision*, pp. 483–494 (2004).
5. K. Kutulakos and E. Steger, "A theory of refractive and specular 3D shape by light-path triangulation," in *Computer Vision, 2005. ICCV 2005. Tenth IEEE International Conference on*, vol. 2, pp. 1448–1455 (2005).
6. D. Miyazaki and K. Ikeuchi, "Inverse polarization raytracing: estimating surface shapes of transparent objects," in *Computer Vision and Pattern Recognition, 2005. CVPR 2005. IEEE Computer Society Conference on*, vol. 2, pp. 910–917 (2005).
7. D. Miyazaki, M. Saito, Y. Sato, and K. Ikeuchi, "Determining surface orientations of transparent objects based on polarization degrees in visible and infrared wavelengths," J. Opt. Soc. Am. A **19**(4), 687–694 (2002).
8. F. Bernardini and H. Rushmeier, "The 3D Model Acquisition Pipeline," in *Computer Graphics Forum*, vol. 21, pp. 149–172 (2002).
9. M. Bertozzi, E. Binelli, A. Broggi, and M. Rose, "Stereo Vision-based approaches for Pedestrian Detection," in *CVPR Workshops, IEEE Computer Society Conference on Computer Vision and Pattern Recognition*, p. 16 (2005).
10. X. Maldague, *Nondestructive Evaluation of Materials by Infrared Thermography* (Springer-Verlag, London, 1993).
11. J. F. Pelletier and X. Maldague, "Shape from heating: a two-dimensional approach for shape extraction in infrared images," in *Optical Engineering*, vol. 36, pp. 370–375 (1997).

12. D. A. Forsyth and J. Ponce, *Computer Vision: A Modern Approach* (Prentice Hall, 2003).
13. J. Phalippou, "Verres. Propriétés et applications," in *Techniques de l'ingénieur. Sciences fondamentales*, vol. AF4, pp. F3601.1–AF3601.19 (2001).
14. J. E. Shelby, *Introduction to glass science and technology* (Royal Society of Chemistry, Cambridge, 2005).
15. R. Siegel and J. R. Howell, *Thermal Radiation Heat Transfer* (Taylor & Francis, 2002).
16. G. Gaussorgues and S. Chomet, *Infrared Thermography* (Springer, 1994).
17. J. Jiao and X. Wang, "A numerical simulation of machining glass by dual CO2-laser beams," in *Optics Laser Technology*, vol. 40, pp. 297–301 (2008).

1. Introduction

Many practical tasks in industry, such as automatic inspection or robot vision, often require scanning of three-dimensional shapes with non-contact techniques. However, transparent objects, such as those made of glass, still pose difficulties for classical scanning techniques.

The reconstruction of surface geometry for transparent objects is complicated by the fact that light is transmitted through, refracted and in some cases reflected off the surface. Tracking refracted scene features might be difficult due to severe magnification or minification of the background pattern. Additionally, if the object is not completely transparent, absorption might change the intensity of the observed features, complicating feature tracking. In the case of reflections, when changing the view point, features appear to move on the surface, no surface feature can be observed directly, and the law of reflection has to be taken into account [1].

Researchers have proposed different approaches to deal with transparent objects. Hata et al. have developed a shape from distortion technique to recover the surface shape of a glass object [2]. They used a structured light setup to project stripe patterns into the object and analyzed distorted patterns, using a genetic algorithm to recover the surface shape. Ben-Ezra and Nayar estimated the parameterized surface shape of transparent objects using structure from motion [3]. Additionally Agarwal et al. presented an extension using optical flow formulations for complex background patterns or irregular transparent objects [4]. Kutulakos and Steger investigated several applications of direct ray measurement and proposed a practical algorithm to reconstruct two interface refractive light interactions using a three-viewpoint setup and measuring the exitant ray directions [5]. Miyazaki et al. have developed a method to determine surface orientations of transparent objects based on polarization degrees in visible and in infrared wavelengths [6, 7]. These approaches can deal relatively well with different sub-classes of objects. However, the algorithms are still very specific and not generally applicable. Furthermore, many techniques require considerable acquisition effort and careful calibration [1].

In this paper, we present a new approach allowing a 3D reconstruction of a given transparent object. The method is based on local surface heating and thermal imaging. The surface of the object is heated with a laser source. A thermal image is acquired, and pixel coordinates of the heated point are calculated. Knowing the internal and external parameters of the acquisition system, the world coordinates are obtained. This process is repeated for several points by moving the object to recover the surface shape of the transparent object. This method is called Scanning From Heating (SFH).

This paper is organized as follows. Section 2 presents the method and its application to transparent glass objects. In section 3, we describe the experimental results, and finally, section 4 concludes the paper.

2. Scanning From Heating (SFH)

There are a variety of techniques, including laser scanners, structured light and time-of-flight, for acquiring 3D models of objects. A good review of 3D model acquisition techniques can be found in [8]. However, most of these methods are designed to obtain the shape of opaque surfaces and are based on analysis of the diffuse (body) reflection component of an objects surface.

These techniques cannot extract models of transparent objects; such objects have only specular (surface) reflection and refraction. Figure 1 illustrates this fact and presents a transparent glass bottle and its reconstruction by a Minolta VI-910 Non Contact 3D Digitizer. The object cannot be properly reconstructed due to reflections and refractions of the projected laser line.

The following section presents SFH, a new approach to recover the 3D surface shape of transparent objects, and discusses the application of the method to glass.

(a) (b)

Fig. 1. (a) Transparent glass bottle. (b) 3D reconstruction by Minolta VI-910 Non Contact 3D Digitizer.

2.1. Description of the method

Thermal images have enjoyed a variety of applications in computer vision. Bertozzi et al. used thermal images and a stereo vision-based algorithm for 3D pedestrian detection [9]. Maldague proposed a method for defect detection by heating the surface and recording a time sequence of thermal images (called thermograms) to observe the temperature decay of the inspected surface [10]. Pelletier et al. also used thermal images to estimate a shape and proposed a 2D approach for shape extraction using a distant uniform heat source [11]. SFH is a new method for 3D shape estimation based on local surface heating by a laser source and observation of it by a thermal camera.

Figure 2 illustrates the method. The transparent object is placed on a moving platform. The laser heat source and the thermal camera are fixed. When the laser fires, the surface of the object is heated at a point.

We assume the following:

- The object surface is opaque to a laser heating source, and laser energy is absorbed by the surface without penetrating into the object.
- Once the surface is heated, the emission of thermal radiation is omnidirectional, so that it can be observed by the thermal camera.

P_1 is the heated point at the surface of the object at Position 1, and (X_1, Y_1, Z_1) are its world coordinates. The projection of P_1 on the camera plane is called P_{c1}, and its coordinates (X_{c1}, Y_{c1}) are in the camera coordinate system (O_c, X_c, Y_c). P_2 is the heated point at Position 2, and (X_2, Y_2, Z_2) are its world coordinates. The projection of P_2 on the camera plane is called P_{c2}, and its coordinates are (X_{c2}, Y_{c2}). The variation of height between P_1 and P_2, ΔZ can be obtained by triangulation using a pinhole camera model [12]:

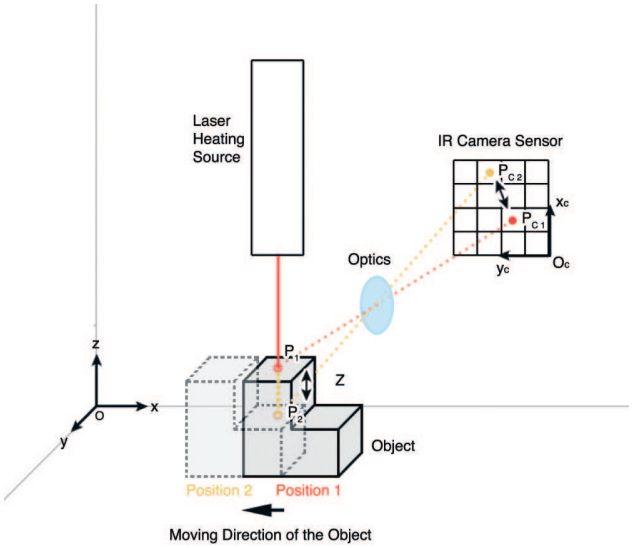

Fig. 2. Scanning From Heating method.

$$\Delta Z = |Z_2 - Z_1| = k.\sqrt{(X_{c2} - X_{c1})^2 + (Y_{c2} - Y_{c1})^2} \tag{1}$$

where k is a constant depending on the intrinsic and extrinsic parameters of the acquisition system. The value of k can be determined by an initial calibration, which consists of determining the camera coordinates of at least two points of a known object. The surface heating process is repeated for several positions of the moving platform, and for each position the 3D coordinates are calculated.

2.2. Application to Glass

Glass is the most commonly used transparent material, and it has many applications in different industries, such as the automotive industry, construction and packaging. Today, with quality becoming increasingly important, each product requires three-dimensional in-line quality control. On the other hand, the difficulties of measuring the surface geometry of transparent materials with actual 3D scanners is a real issue for industrial vision. This section reviews transparency and emissivity of glass and discusses the application of SFH.

2.2.1. Transparency

Transparency of glass is a fact related to optical transmission defined by Beer Lamberts law:

$$\frac{I}{I_0} = \exp(-\alpha x) \tag{2}$$

I_0 is the intensity of the entering beam into a volume of glass with a depth x, I is the intensity of the emergent beam, and α is the absorption coefficient, which is defined by:

$$\alpha = \frac{4\pi}{\lambda} K(\lambda) \tag{3}$$

with $K(\lambda)$ being the absorption index and λ being the wavelength [13]. Figure 3 presents the evolution of the absorption index of glass depending on the wavelength. Absorptions are located in the UV domain and infrared domain of the spectrum.

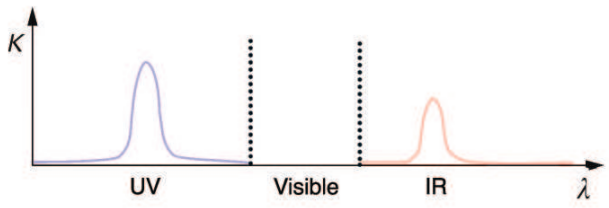

Fig. 3. Evolution of the absorption index of glass depending on the wavelength [13].

Figure 4 illustrates the transmission of light as a percentage in the infrared domain of most commonly used glasses. For each type, there is a wavelength such that the transmission is close to 0%. This wavelength is called the infrared cut-off, and it depends on the composition of the glass [14]. At a wavelength higher than $10\mu m$, the glasses presented in Figure 4 can be considered as opaque objects. Figure 5 illustrates this fact and shows an image of a SiO_2 glass bottle, placed in front of an infrared illumination and observed with a long wave infrared camera sensitive to $8-13\mu m$. The object does not transmit the light coming from the source and appears to be opaque.

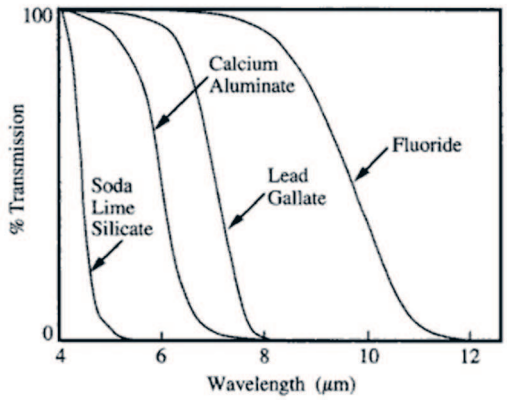

Fig. 4. Transmission of light as a percentage in the infrared domain of commonly used glasses [14].

2.2.2. Emissivity

All substances continuously emit electromagnetic radiation because of the molecular and atomic agitation associated with their internal energy, which is proportional to the material temperature. Emissivity specifies how well a real body radiates energy compared to an ideal body, called a blackbody. A blackbody is considered a perfect absorber and emitter in each direction at every wavelength. For the SFH method to work properly, the emission of the thermal radiation of the heated object should be omnidirectional. If not, only the parts of the surface with an angle to the camera, where the emissivity is high, can be observed and reconstructed. Unfortunately, unlike the intensity from a blackbody i_b, the intensity emitted from a real body

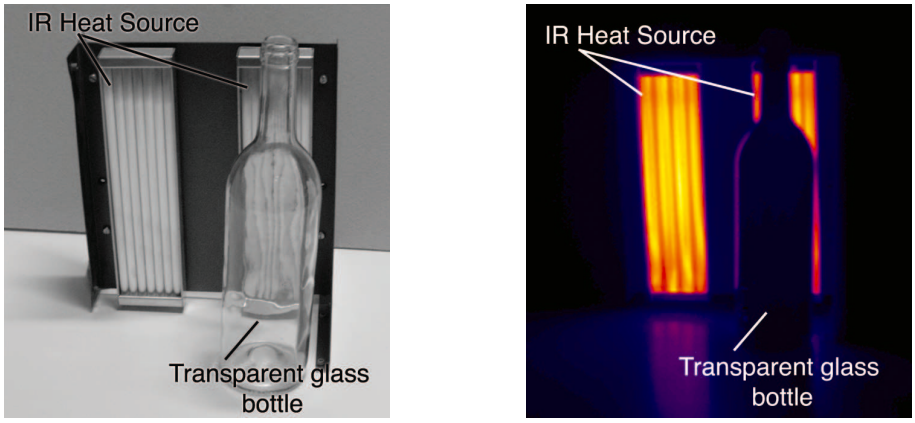

(a) (b)

Fig. 5. (a) Transparent glass bottle in front of an infrared heat source. (b) Image taken with a long wave infrared camera sensitive to $8-13\mu m$.

i depends on direction. The emissivity of a real surface dA of temperature T_A per unit time in wavelength interval $d\lambda$ and within the solid angle (θ, φ) is given by [15]:

$$\varepsilon(\lambda, \theta, \varphi, T_A) = \frac{i(\lambda, \theta, \varphi, T_A)}{i_b(\lambda, \theta, \varphi, T_A)} \tag{4}$$

Figure 6 illustrates the angular emissivity of a dielectric sphere like glass. The radiation approaches a lambertian source. Consequently, the SFH method can be applied to glass objects with negligible losses.

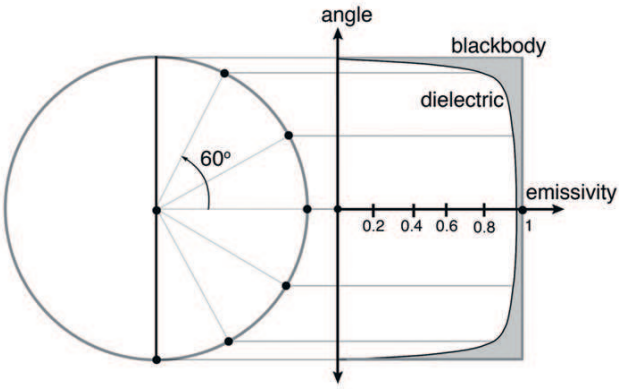

Fig. 6. Emissivity of a dielectric sphere [16].

2.2.3. Conclusion

To conclude, the emissivity of glass approaches an omnidirectional source, and the SFH method can be applied to glass. For transparent glass objects, a laser heat source working at a wavelength higher than $10\mu m$ is suitable. The object surface is then opaque to the laser heating source, and the laser cannot penetrate into the object, causing only a local surface heating. We propose to use a CO_2 laser at $10.6\mu m$.

3. Implementation

3.1. Experimental Setup

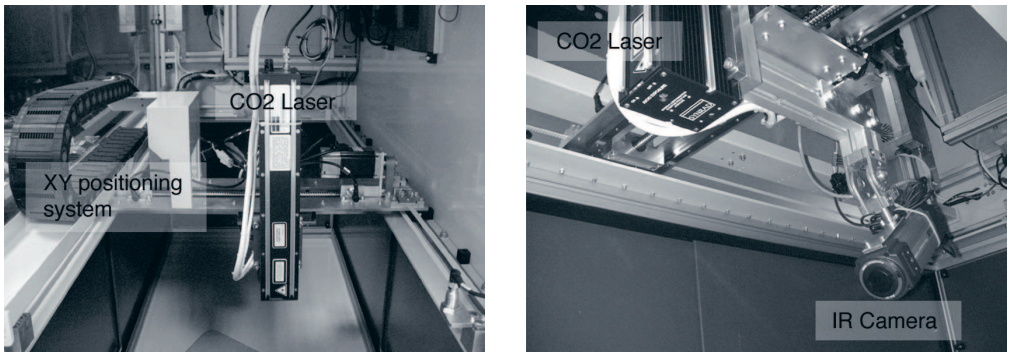

(a) (b)

Fig. 7. (a) XY positioning system. (b) CO2 laser and IR camera, fixed on the positioning system.

Figure 7 shows the experimental setup. A Synrad 48 Series $10W$ CO_2 Laser at $10.6\mu m$ is used as the heating source. Thermal images are acquired with a Flir A320G LWIR Camera sensible to $8-13\mu m$. The power of the laser is controlled by a Synrad UC2000 Laser Power Controller. The laser and the thermal camera are placed on a moving platform, and the object is fixed. The XY positioning system is programmable to scan a given area in predefined steps in X and Y, with a precision of $50\mu m$. Additionally, the laser is set to fire continuously as it moves over the object, making it possible to acquire thermal images without stopping and to recover 3D points at the maximum speed of the camera (50fps).

3.2. Predetermination of the Laser Power

Reconstruction in the SFH method is based on detecting the heated point at the surface of the object. In reality, the laser beam has a given radius ($1.5mm$ for the experimental setup), and detection is complicated by the fact that the laser irradiation is observed as a surface heating zone and not a point. Additionally, the prediction of the laser power, to bring the surface of the object to a given temperature, is crucial to obtain a detectable heat zone without damaging the surface. To predict the laser power and the heat distribution of the laser irradiation zone, we apply a mathematical model proposed by Jiao et al. for a glass plate heated axisymmetrically by a CO2 laser [Fig. 8] [17].

For a laser beam traveling in direction x at a constant velocity v, we consider the laser power to have a Gaussian distribution as in Eq. (5). We treat the CO_2 laser beam as a surface heating source, so the impulse function $\delta(z)$ is applied in Eq. (5).

$$I(x,y,z,t) = \frac{P_0}{\pi r^2} \exp\left(-\frac{(x-vt)^2+y^2}{r^2}\right)\delta(z) \tag{5}$$

where P_0 and r are the power and the radius of the CO_2 laser beam, respectively.

Figure 9 presents the prediction of the model to heat a glass plate with an ambient temperature of 20°C to 80°C. The CO2 laser has a focus of 1.5mm (half width), and the movement speed of the system is set to 10mm/second. The model predicts the laser power as 3W. The experimental results obtained with the same configuration and a 3W laser are also shown in Figure 9.

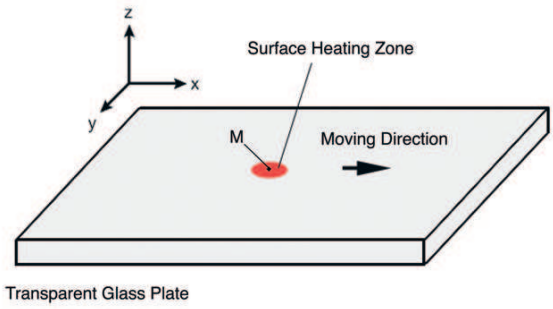

Fig. 8. Heating model.

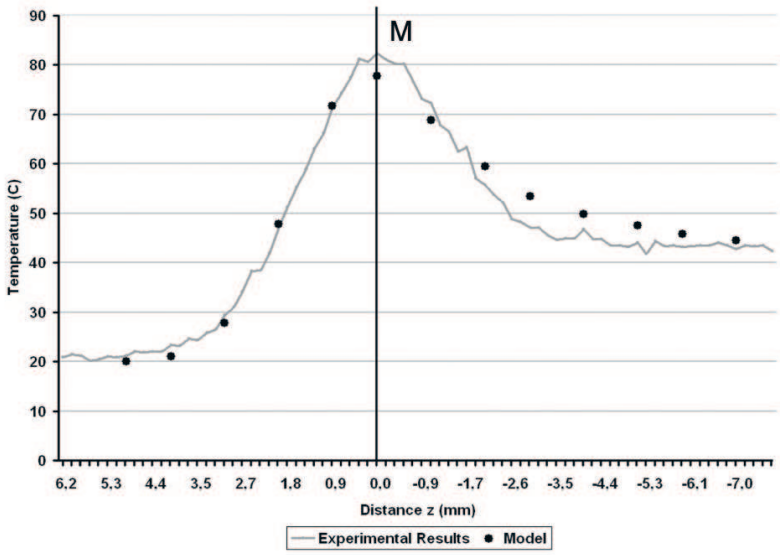

Fig. 9. Experimental results compared to the heating model.

The experimental results fit the model reasonably. The surface temperature increases rapidly when the glass enters the heating region. The temperature reaches its peak at a position at the center of laser irradiation, where the highest laser intensity is imposed. Then it decreases sharply due to a high rate of cooling by radiation, air convection and conduction into the glass.

3.2.1. Detection of the laser irradiation

After section 3.2, the temperature reaches its peak at the center of laser irradiation P_c. On the thermal image, P_c corresponds to the point with the highest intensity. As thermal images are low resolution (320x240 pixels) and noisy, to obtain the pixel coordinates of P_c, we first smooth the image with a Gaussian filter of 11x11 pixel size and $\sigma = 2.36$. Then, at each point, the input image is approximated by a quadratic polynomial in x and y, and subsequently, we examine the polynomial for local maxima [Fig. 10]. Once the maxima is determined, we recover the world coordinates of the surface point using Eq. (1). We repeat the operation for each thermal image, for different positions of the moving platform, to obtain surface reconstruction of the object.

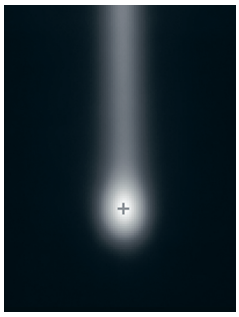

Fig. 10. Result of Gaussian filter and maxima detection on the thermal image.

3.3. Results

The following paragraphs present the results obtained from the experimental setup. In order to validate the efficiency and to determine the accuracy, we first apply the method to a glass plate. Then, we scan a glass window used in the automotive industry to evaluate the performance on real objects. Finally, to see the possibilities of extension to other materials, we present the application of the method on a transparent plastic bottle.

3.3.1. Transparent glass plate

Figure 11 illustrates the results obtained on a 10x5cm glass plate from 65 points. The distance between the camera and the plane is set to $50cm$. The histogram of the deviation between the results and a perfect plane is also presented. The average deviation is $150\mu m$. This deviation is quite significant and permits us to validate the efficiency of the method.

3.3.2. Automotive window glass

Figure 12 illustrates a glass window used in the automotive industry and its reconstruction by a probe scanner. Additionally, we present the comparison to the reconstruction by the SFH method. The density of reconstruction obtained by the probe scanner (200 points) is much smaller than the reconstruction obtained by SFH measurement (6000 points). The interpolation of the point cloud obtained with the probe scanner increases the estimated error. The average deviation between the two reconstructions is $360\mu m$.

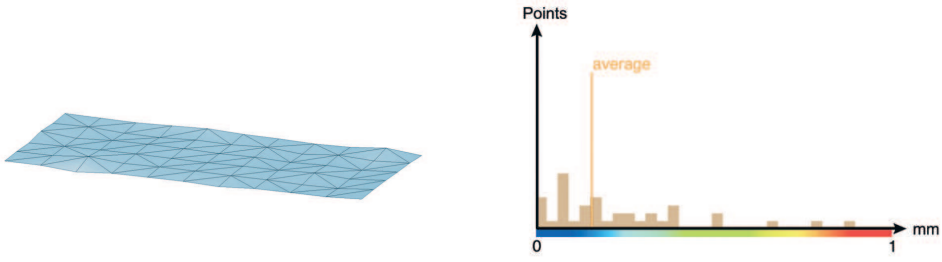

(a) (b)

Fig. 11. (a) Reconstruction of a glass plate by the SFH method. (b) Histogram of the deviation between the results and a perfect plane.

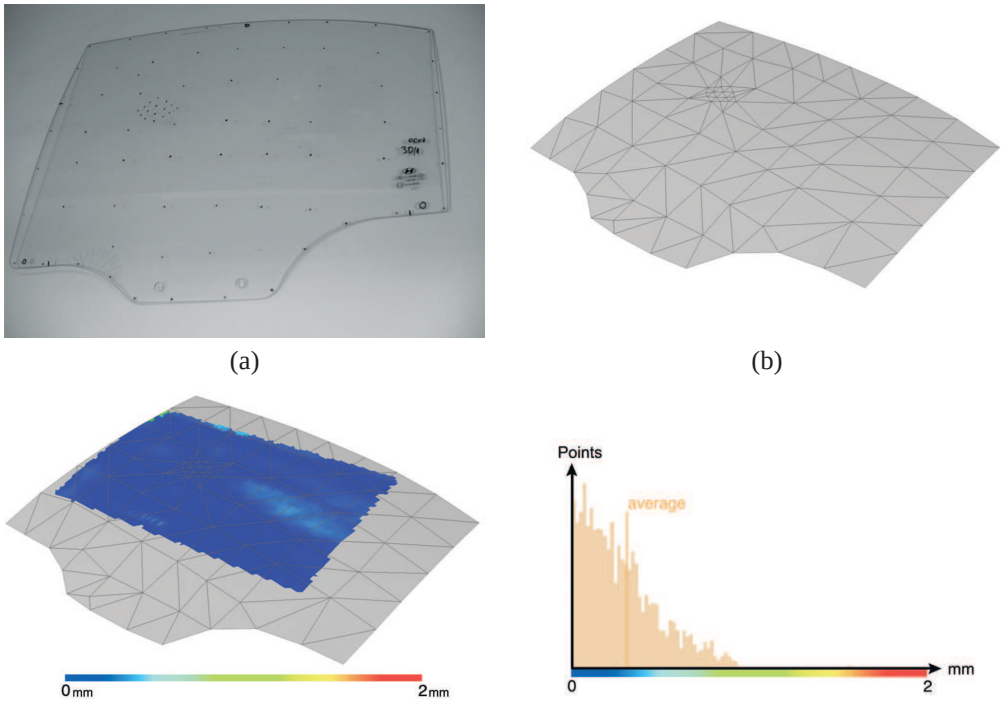

(a) (b)

(c) (d)

Fig. 12. (a) Glass window used in the automotive industry. (b) Reconstruction of the glass window by a probe scanner. (c) Reconstruction of the glass window by a probe scanner, partially compared to the reconstruction by SFH method. (d) Histogram of the difference between two reconstructions.

3.3.3. Application to plastic

It is also possible to apply the SFH method to different transparent materials. Figure 13 illustrates 3D reconstruction of a plastic bottle by the SFH method and compares the result to the 3D reconstruction obtained by a Minolta VI-910 Non Contact 3D Digitizer of the same bottle, powdered on the surface. The results fit reasonably well, and the average deviation is $200\mu m$. Differences between the two models are mostly located on the borders of the scanning region and are probably due to calibration errors in both reconstruction systems.

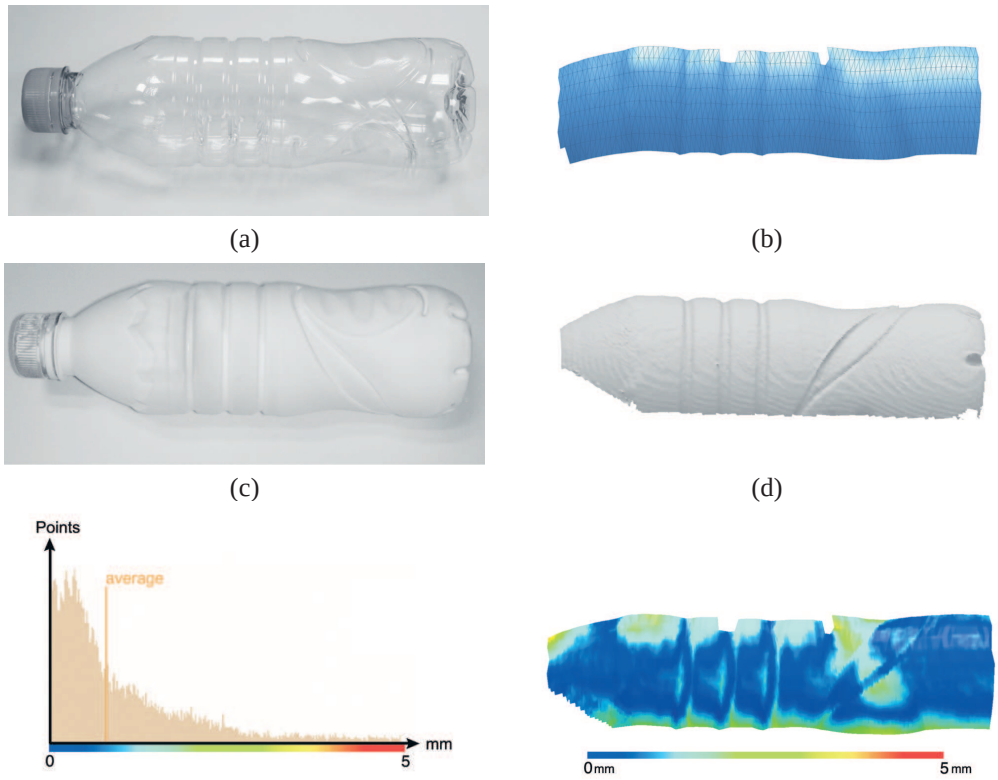

Fig. 13. (a) Transparent plastic bottle. (b) Reconstruction obtained by the SFH method. (c) Powdered plastic bottle. (d) Reconstruction of powdered bottle obtained by a Minolta VI-910 Non Contact 3D Digitizer. (e) Histogram of the difference between the two reconstruction. (f) 3D representation of the difference between the two reconstructions.

4. Conclusion

The 3D reconstruction of transparent objects is a very difficult problem in computer vision due to transparency and specularity of the surface. Classical methods based on triangulation in the visible domain are not efficient.

This paper proposes a new method, called Scanning From Heating (SFH), to determine the surface shape of transparent objects using laser surface heating and thermal imaging. When the object is opaque to the laser source, the surface is heated at the impact zone. The laser irradiation is observed with an infrared camera, and 3D coordinates of the surface at that point are computed using triangulation and the initial calibration of the system. Furthermore, we

discussed the implementation and presented results on different surface shapes.

The results obtained on glass objects are promising. While we have studied only the application to transparent glass, the results show that extension to other transparent materials, such as plastic, is possible.

Future work includes the design of an experimental system that can project a specific pattern (line, grid, matrix of points, etc.) to improve the 3D point acquisition speed. We will also study the application to different materials (effects on the reconstruction, laser type and power), and finally, we envisage an industrial prototype.

Acknowledgments

We gratefully acknowledge the help of C. Oden, H. Isik, E. Dogan and G. Ciftci from Vistek A.S., M. Akay, H. Yuksek and H. Yavaslar from Sisecam A.S., E.D. Kunt and K. Cakir from AMS and O. Aygun from Flir Systems Turkey. This project was partially supported by SANTEZ(00335.STZ.2008-2) and SPICE(FP6-2004-ACC-SSA-2).